# Effect of bending stiffness of the electroactive polymer element on the performance of a Hybrid Actuator System (HYBAS)

Tian-Bing Xu[1], Ji Su[2], Xiaoning Jiang[3], Paul W. Rehrig[3], Shujun Zhang[4], Thomas R. Shrout[4], and Qiming Zhang[4]

[1]National Institute of Aerospace, 144 Research Drive, Hampton, VA 23666, USA
[2]NASA Langley Research Center, Hampton, VA 23681, USA
[3]TRS Technologies, Inc., 2820 East College Avenue, State College, PA 16801, USA
[4]Materials Research Institute, The Pennsylvania State University, University Park, PA 16802

## ABSTRACT

An electroactive polymer (EAP)-ceramic hybrid actuation system (HYBAS) was developed recently at NASA Langley Research Center. This paper focuses on the effect of the bending stiffness of the EAP component on the performance of a HYBAS, in which the actuation of the EAP element can match the theoretical prediction at various length/thickness ratios for a constant elastic modulus of the EAP component. The effects on the bending stiffness of the elastic modulus and length/thickness ratio of the EAP component were studied. A critical bending stiffness to keep the actuation of the EAP element suitable for a rigid beam theory-based modeling was found for electron irradiated P(VDF-TrFE) copolymer. For example, the agreement of experimental data and theoretical modeling for a HYBAS with the length/thickness ratio of EAP element at 375 times is demonstrated. However, the beam based theoretical modeling becomes invalid (i.e., the profile of the HYBAS movement does not follow the prediction of theoretical modeling) when the bending stiffness is lower than a critical value.

Key words: hybrid actuator system (HYBAS), bending stiffness, electroactive polymer (EAP), actuation

## 1. INTRODUCTION

The concept of hybrid actuation system (HYBAS) recently developed at NASA Langley research center[1, 2]. The HYBAS demonstrates a significantly-enhanced electromechanical performance by utilizing the advantages of synergistic contributions of the electromechanical responses of an EAP and of an electrostrictive single crystal. The development of HYBAS does not only provide a high performance electromechanical actuation system, but also proves an innovative concept for future and more extensive applications in the development of next generation of electromechanical actuators. The HYBAS offers several advantages which include following: 1) A HYBAS can offer significantly-enhanced displacement when compared with that given by each of the element individually. 2) Enhanced electromechanical output power. A HYBAS can enhance the electromechanical output power by simultaneously actuating both elements by a single power supply. Therefore the electromechanical output power is higher than that generated by each element individually. 3) Adjustability in configuration design. The design of each active element and the combination of the two active elements can be tailored to meet the requirements for a HYBAS in different applications. The requirements can be of the electromechanical output power, the driving voltage, the maximum displacement, etc. 4) The concept of a HYBAS combines advantages of flextensional transducers/actuators[3] and Thunder transducers/actuators[4].

In order to optimize the performance of a HYBAS, a theoretical model has been developed, based on the elastic and electromechanical properties of the materials, and based on the configuration of the device[5]. Previous research demonstrated that the model and the experimental results show good agreement and validate the model as an effective method for the further development of high-performance actuating devices and systems for various applications.

This paper will focus on the investigation of the bending strength effect of the EAP component on the performance of a HYBAS, in which the actuation of the EAP element can match the theoretical prediction, at various geometries for a constant elastic modulus of the EAP component.

## 2. ELECTROACTIVE POLYMER-CERAMIC HYBAS

In general, the transverse strain is negative and longitudinal strain positive in inorganic materials, such as ceramics/single crystals. However, the transverse strain is positive and longitudinal strain negative in electroactive polymer (EAP). The proven HYBAS, concept is to utilize the properties of different strain directions in each single element to enhance the performance of a designed transducer/actuator system for underwater transductions, mechanical motion controls, and other applications such as optical scanners for warfare, position controls for intelligent facilities, and flow dynamic controls.

The cross sectional view of the HYBAS configuration for this investigation is illustrated schematically in Fig. 1. Two constituent materials were used in the investigation. The electroactive polymer (EAP) was the uniaxially-stretched and high energy electron-irradiated 68/32 mol.% poly(vinylidene fluoride-trifluoroethylene) [P(VDF-TrFE)] copolymer in the form of a film, and electrostrictive single crystal (ESC) compoment was the Rhombohedral <001> oriented $Pb(Zn_{1/3}Nb_{2/3})O_3$-4.5%$PbTiO_3$ crystal (<001> oriented PZN-4.5%PT), PZN-PT single crystal. The EAP film was prepared as discussed in references 6 and 7. The ESC beam was prepared as discussed in reference 8. Both constituent materials offer a high transverse electrostrictive strain. However, the directions of the electric field-induced strain responses of the two materials are opposing [6, 8].

Two pieces of plastic rods, which served as a frame to hold the single crystal and the EAP components, were bonded to the two ends of the ESC beam with epoxy. The effective length of the HYBAS was defined by the length of the ESC component. The EAP element used was a bi-layered actuator formed with a 16 μm thick active layer bonded to an inactive layer (same polymer) using Spurr epoxy (Polysciences, Inc., Warrington, PA). The active layer of the EAP film was coated with 0.1μm gold electrodes on both sides with shadow mask to serve as electrodes and also as a reflection mirror for displacement characterization. The EAP element was bonded onto the plastic frames using epoxy. The inactive layer should act as a direction controller to guide the motion of the EAP actuation element when it is activated electrically. The small gap between the EAP and the ESC beam was for easy processing control and characterization. The space of the gap could be varied as needed for different applications. The electric connection for the system needs one electric power source to drive both actuation elements at the same time, or drive each of the elements individually as needed.
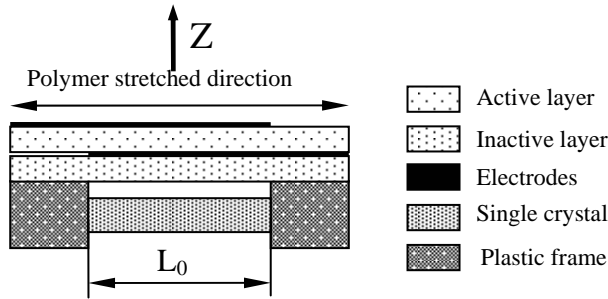


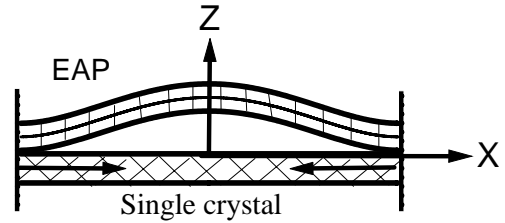Fig. 1. Schematic of the cross section view of the HYBAS investigated.



Fig. 2. Schematic of the actuation responses of the HYBAS under the applied electric field: the actuator moves upward from the neutral position (z=0) since the transverse strain in the active layer $S_1>0$.

In order to improve the using ability of HYBAS, it was modified as shown in Fig. 3. The center plastic beam is used to hold the actuator to improve the application capability of the HYBAS. The modified HYBAS can be fitted to various applications due to the central plastic beam, which is used to access the connection to other devices.
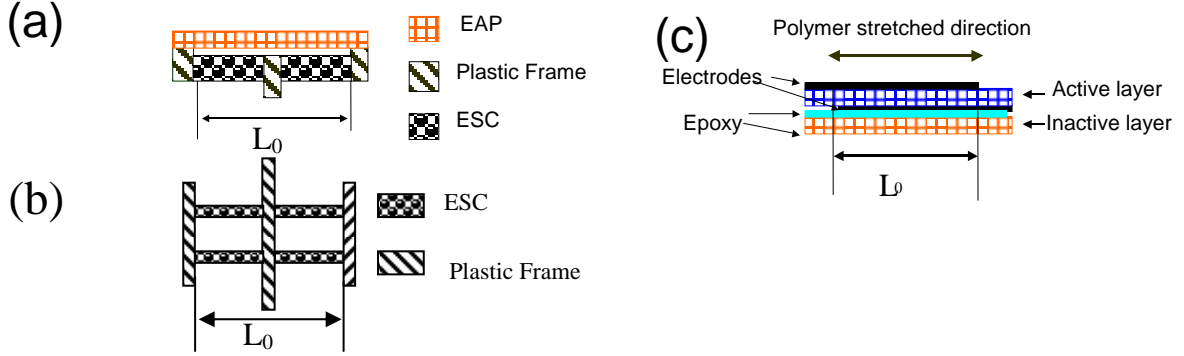


Fig. 3. Diagram of modified HYBAS. (a) The schematic structure of the HYBAS (Front view). (b) Diagram of the ESC component with plastic frame (Top view) (C) Diagram of the EAP component (Front view).

## 3. HYBAS PERFORMANCE MODELING AND DESIGNS

The device was modeled as a rectangular plate under uniform mechanical pressure in the vertical direction ($z$) as shown in Fig. 1. Since the elastic modulus of the ESC (20 GPa)[10] is much higher than the elastic modulus of the EAP (1GPa)[9] and the cross sectional area of the ESC is 10 times larger than the polymer component, the dynamic length of HYBAS, $L'_0$, is dominated by the ESC component. It can be expressed as

$$L'_0 = L_0(1 + (-S^e_{ESC}))$$
(1)

where $L_0$ is the total initial length of the ESC, i.e., the effective length of the HYBAS when the electric field is zero, $S^e_{ESC}$ is the magnitude of the effective electrostrictive strain of the ESC, which is a function of electric field, and the "-" indicates the strain in the ESC is negative in the transverse direction.

Since the thickness, $t$, of the EAP component is much less than the length $L_0$ of the device, we assume that the thickness of the active layer of the EAP component will not change during operation. When an electric field is applied to the device, the active polymer layer will expand along the stretched direction. Meanwhile, the inactive layer constrains the motion of the active layer. This interaction will result in a uniform load distributed on the rectangular plate (or beam) with both ends fixed. The ESC component acts as a contractive force on the two ends of the plate. The force on the two ends of the EAP plate will enhance the movement in the $z$-direction, since the plate is bending in the $z$-direction under the load at the same time. This actuation process is schematically shown in Fig. 2 and the displacement ($w$) in the $z$ direction of the HYBAS as a function of $x$ can be expressed as [11]

$$w = c\left(\left(\frac{L'_0}{2}\right)^2 - x^2\right)^2$$
(2a)

and

$$c = \frac{W}{24EI}$$
(2b)

where $W$ is equal to the uniformly distributed load per unit length (dependent on the strains of the EAP and the ESC components), $E$ is Young's modulus of the EAP component (since both layers have the same elastic modulus), $I$ is the moment of the inertia of the plate, and $x$ is the position along the beam (see Fig. 2).

Assuming that the effective strain of the EAP component in the plate $(x)$ is $S^e_{EAP}$, then, the total length $L$ of the curved plate due to the strain $S^e_{EAP}$ is

$$\int_{-\frac{L'_0}{2}}^{\frac{L'_0}{2}} \sqrt{c^2\left(4x^3 - L_0^2(1-S^e_{ESC})^2 x\right)^2 + 1} \cdot dx = \left(1 + S^e_{EAP}\right)L_0 \tag{3}$$

Clearly, the parameter $c$ is directly related to both the strains in the ESC component ($S^e_{ESC}$) and in the EAP component ($S^e_{EAP}$). Equation (3) can be solved to give the parameter $c$ as a function of the initial length and the strains. The displacement $w$ as a function of $x$ can be calculated by inserting the parameter $c$ into Eqs. (2a). The detail of the modeling was described in reference 5.

The effective strain in the EAP component can be expressed as[5]

$$S^e_{EAP} = \frac{S_0}{1+k} \tag{4}$$

Where $S_0$ the free strain in the freestanding active layer in the free condition, and $k$ is referred to as the clamping ratio, which is a measure of the clamping effect, due to the inactive layer, the epoxy layer, the unelectroded edges of the active layer, as well as the metal electrodes layers. The clamping ratio can be expressed as

$$k = \frac{E^e_n t^e_n b^e_n}{E_a t_a b_a} = \frac{\sum_{i=1}^{n} E_{ni} t_{ni} b_{ni}}{E_a t_a b_a} \tag{5}$$

where $E^e_n, t^e_n$, and $b^e_{ni}$ are the equivalent of Young's modulus, thickness, and width of active layer; and $E_{ni}$, $t_{ni}$ $b_{ni}$ are Young's modulus, thickness and width of the *ith* inactive layer.

Based on the theoretical modeling, examples of displacement profiles for HYBAS actuators with different lengths at 800 $V_{rms}$ is presented in Fig. 4. The displacement can reach 1.6 mm for a 40 mm long HYBAS at this voltage if the same thickness is maintaining for the two actuation components (i.e., electroactive polymer and electrostrictive single crystal).
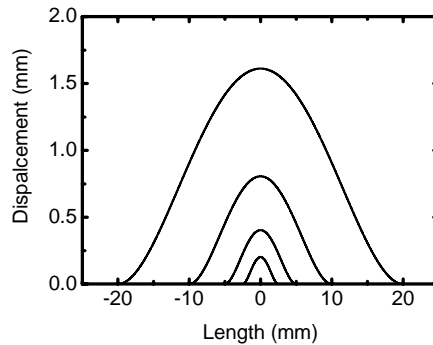


Fig. 4. Calculated displacement profiles for HYBAS actuators with different lengths at 800 Vrms. From top to bottom for HYBAS with length at 40 mm 20 mm, 10 mm, and 5 mm, respectively.

The calculated center (maximum) displacement as a function of length for HYBAS actuators at different voltages applied is shown in Fig. 5. The displacement can reach 2.9 mm when 1370 $V_{rms}$ is applied to a 50 mm long HYBAS. The calculated results indicate that it is possible to generate a displacement around 2 mm for a HYBAS with a 40 mm long.
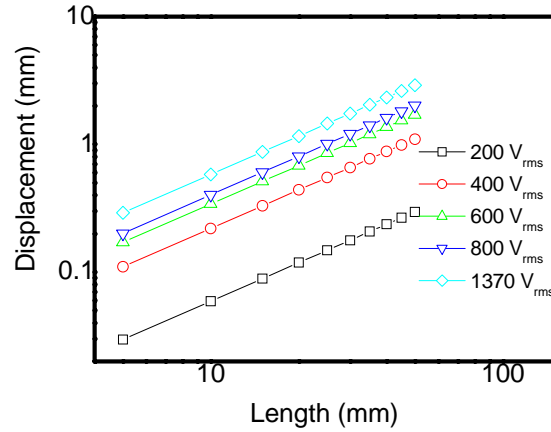


Fig. 5. Calculated center displacement as a function of length for HYBAS at different voltages.

## 4. CHARACTERIZATION AND PERFORMANCES OF HYBAS IN DIFFERENT LENGTH

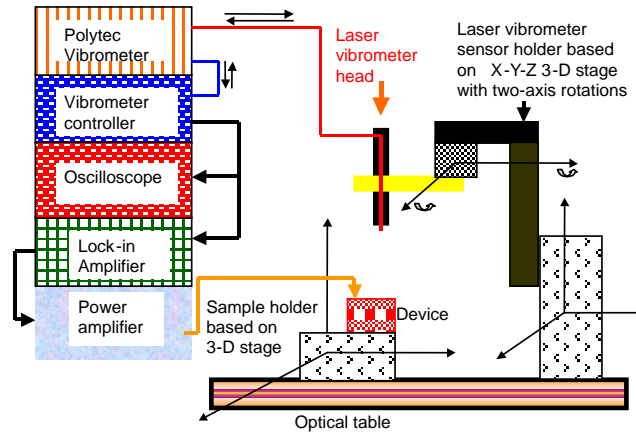### 4.1 Characterization set up for displacement measurement



Fig. 6 Diagram of displacement characterization set-up for HYBAS.

The diagram of the displacement measurement setup was shown in Fig. 6. The HYBAS was mechanically fixed on a test fixture-based on a 3-D stage. The displacements were measured utilizing a laser vibrometer (Polytec PI, Inc., model OFV-512) at room temperature. The laser vibrometer head was attached on a 3-D travel and a 2-D rotation stages based sensor holder in order to adjust the laser beam to perpendicular to the measured surface of the device. In order to increase the resolution of the laser vibrometer, a lock-in amplifier was used to pickup the signal. Combining with a lock-in amplifier, the displacement resolution of the laser vibrometer system can go down to 0.5 nm.

## 4.2  A HYBAS with 5.5 mm effective length

The parameters of the components of a 5 long HYBAS are listed in Table 1. The detail of the HYBAS was described in references 2 and 5.

Table 1. Dimension parameters of the device and elastic modulus of the materials used

| Parameters / Materials | Length (mm) | Thickness (µm) | Width (mm) | | Elastic modulus (GPa) |
|---|---|---|---|---|---|
| | | | Total | Effective | |
| PZN-PT single crystal elements | 5.50 | 470.0 | 3.00 | 3.00 | 20.0 |
| Active EAP layer | 5.50 | 16.0 | 4.50 | 3.00 | 1.0 |
| Edges of active layer(2) | 5.50 | 16.0 | 0.75 | 0.75 | 1.0 |
| Inactive EAP layer | 5.50 | 15.0 | 4.50 | 4.50 | 1.0 |
| Spurr epoxy layer | 5.50 | 1.0 | 4.50 | 4.50 | 5.0 |
| Au electrodes on both side of active EAP | 5.50 | 0.1 | 4.50 | 4.50 | 74.0 |

The driving voltage applied was AC at 10 Hz and the HYBAS displacement was detected as a second harmonic (electrostrictive) response.  Fig. 7 presents the displacement profiles of the device at 400 $V_{rms}$ (the peak electric field of 1.2 V/µm for the ESC component and 35.4 V/µm for the EAP component).  Fig. 7 demonstrates that the experimental results and the results from the theoretical model demonstrate good agreement.  The center displacement as a function of the applied voltage is shown in Fig. 8.  The displacement is 214 µm at 800 $V_{rms}$.
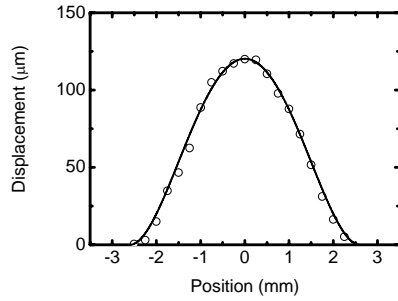


Fig. 7 The displacement profiles on a HYBAS as a function of $x$ for AC driving voltage (10Hz) at 400$V_{rms}$ (Electric field of 1.2V/µm for single crystal and 35.4V/µm for EAP), respectively.   The dots are measured results.  The solid lines are modeling results.
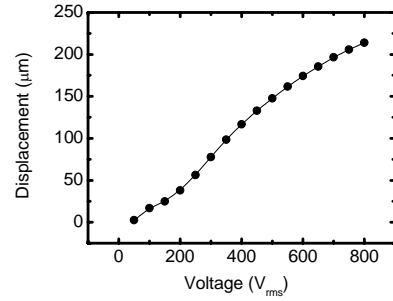


Fig. 8. Displacement at the center of a HYBAS as a function of the applied AC voltage (10 Hz) where symbols are the experiment data and the solid lines are a guide for the eyes.

## 4.3  A HYBAS with 12 mm effective length

The diagram of a HYBAS with 12 mm effective length is shown in Fig. 3.  The parameters of the device are listed in table 2.

The measured and theoretically modeled displacement profiles for the 12 mm long HYBAS at 300 $V_{rms}$ and 1 Hz driving signal is shown in Fig. 9. The circular dots show measured data and the solid line represents the modeling result. The agreement between the modeling result and the measured data indicates the EAP element is still in the rigid state when the 12 mm long HYBAS with length thickness ratio at 375 times. The center displacement as a function of the applied voltage is shown in Fig. 10. The displacement is 259 μm at 600 $V_{rms}$.

Table 2. Dimension parameter of the HYBAS and the elastic modulus of the materials used

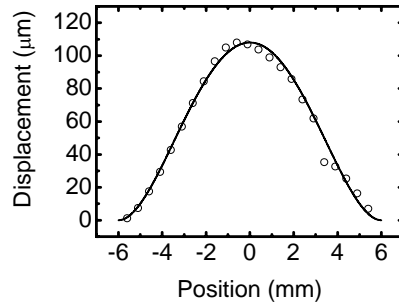| Parameters <br> Materials | Length (mm) | | Thickness (μm) | Width (mm) | | Elastic modulus (GPa) |
|---|---|---|---|---|---|---|
| | Total | Effective | | Total | Effective | |
| PZN-PT single crystal element | 12.0 | 10.5 | 500 | 3.0 | 3.0 | 20 |
| Active EAP layer | 12.0 | 12.0 | 16 | 14.5 | 12.5 | 1 |
| Edge of active EAP layer (2) | 12.0 | 12.0 | 16 | 1.0 | 1.0 | 1 |
| Inactive EAP layer | 12.0 | 12.0 | 16 | 14.5 | 14.5 | 1 |
| Spurr epoxy layer | 12.0 | 12.0 | 1 | 14.5 | 14.5 | |
| Au electrode on | 12.0 | 12.0 | 0.07 | 12.5 | 12.5 | 74 |



Fig. 9. Displacement profiles for 12 mm long HYBAS at 300 $V_{rms}$ 1 Hz (o = measured data, — modeling result)
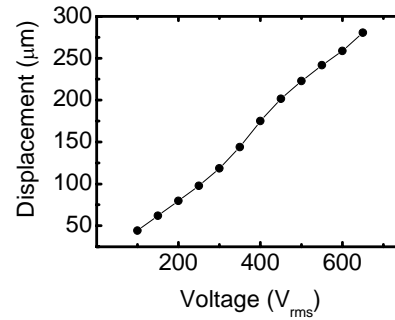
Fig. 10. Center displacement versus voltage for 12 mm long HYBAS at 1 Hz

## 4.4. A HYBAS with 41 mm effective length

The diagram of a 41 mm long HYBAS is also as described in Fig. 3. Parameters of the device are listed in table 3.

The displacement profiles for a 41 mm long HYBAS at 500 $V_{rms}$ and 700 $V_{rms}$, with 1 Hz AC frequency is shown in Fig. 11. Dots are measured data and solid lines are modeled results for the HYBAS. The mismatch between modeling results and measured data indicates that the EAP element is out of the rigid state for a single layer EAP active polymer in such long HYBAS due to the length/thickness ratio, which is too high (1250 times). Since the performance of 12 mm long HYBAS has very good agreement with the theoretical modeling at same thickness (active layer + inactive layer+ epoxy = 33 μm) with length/thickness ratio of 375 times, it is expected that the EAP component of the 41 mm long HYBAS will work at rigid state; that is the experimental result will agree with the theoretical modeling result, when the total thickness of the EAP component is over 100 μm. A multilayer polymer stack should replace the single layer element to keeping it in rigid state and increase the load capability of the HYBAS. The center displacement as a function of the

applied voltage is shown in Fig. 12. The displacement is 880 μm at 800 $V_{rms}$. The center displacement will be over 1 mm at 800 $V_{rms}$ if the HYBAS work at rigid state.

Table 3. Dimension parameters of the HYBAS and the elastic modulus of the materials used

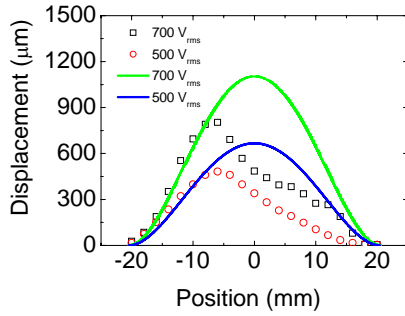| Parameters Materials | Length (mm) | | Thickness (μm) | Width (mm) | | Elastic modulus (GPa) |
|---|---|---|---|---|---|---|
| | Total | Effective | | Total | Effective | |
| PZN-PT single crystal element | 41.0 | 40 | 1000 | 5.0 | 5.0 | 16.8 |
| Active EAP layer | 41.0 | 41.0 | 15 | 14.5 | 12.5 | 1 |
| Edge of active EAP layer (2) | 41.0 | 41.0 | 15 | 1.0 | 1.0 | 1 |
| Inactive EAP layer | 12.0 | 12.0 | 16 | 14.5 | 14.5 | 1 |
| Spurr epoxy layer | 12.0 | 12.0 | 2 | 14.5 | 14.5 | |
| Au electrode on | 12.0 | 12.0 | 0.07 | 12.5 | 12.5 | 74 |



Fig. 11. Displacement profiles for 41 mm long HYBAS at 500$V_{rms}$ and 700$V_{rms}$ 1 Hz. The dots are measured results. The solid lines are modeling results.
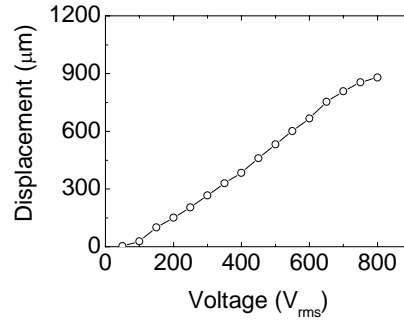
Fig. 12. Center displacement versus voltage for 41 mm long HYBAS at 1 Hz

## 5. CONCLUSIONS AND RECOMMENDATIONS

In summary, based on the theoretical model, the performances of the HYBAS with different lengths were predicted. According to the theoretical predictions, three HYBASs with different lengths were designed, prototyped, and characterized. The displacement profiles, as well as the center displacement versus applied voltage of the three HYBASs were characterized. The measured displacement profiles of the 5.5 mm and 12 mm long HYBASs matched well with the theoretical prediction. However, there is some degree of mismatch between the modeled result and the measured result for the 41 mm long HYBAS. The mismatch indicates that the EAP element is out of the rigid state for a single active EAP layer in such a long HYBAS due to the length/thickness ratio, which is too high (1250 times). The critical bending stiffness for EAP component with modulus at 1 GPa will be at the length/thickness ratio over 375 times.

Since the performance of 12 mm long HYBAS has very good agreement with the theoretical modeling at the same thickness with length thickness ratio at 375 times, it is expected that the EAP component of the 41 mm long HYBAS will work at rigid state; that is the experimental result agrees with the theoretical modeling result, when the total

thickness of the EAP component is over 100 μm. A multilayer polymer stack should replace the single layer element to keep it in a rigid state and increase the load capability of the HYBAS.

## 6. ACKNOWLEDGEMENTS

## 7. REFERENCES

1.  J. Su, and T.-B. Xu, Disclosure filed, *LAR-16698-1, August, 2003*
2.  J. Su, T. Xu, S Zhang, T. Short, and Q.M. Zhang, "A electroactive polymer-Ceramic Hybrid Actuation System for Enhanced Electromechanical Performance," Accepted by *Appl. Phys. Lett.* 85 (6), 1045 (2004).
3.  R. E. Newnham, Q.C. Xu, and S. Yoshikawa, "Transformed stress direction acoustic transducer," *United State Patent*, # 4,999,819, 1991, and "Metal-electroactive ceramic composite actuators," *United State Patent*, # 5,276,657, 1994
4.  Richard F. Hellbaum, Robert G. Bryant, and Robert L. Fox, "Thin layer composite unimorph ferroelectric driver and sensor," *United State Patent* # 5,632,841; R. Bryant, "Process for preparing a tough, soluble, aromatic, thermoplastic copolyimide," *United State Patent* # 5,639,850; Face International Thunder page: http://www.face-int.com/thunder/thunder.htm
5.  Tian-Bing Xu, and Ji Su, "Theoretical Modeling on Electroactive Polymer-Ceramic Hybrid Actuation Systems," Journal of Applied Physics 97(3), 034908, 2005.
6.  Z. -Y. Cheng, V. Bharti, T. Mai T. -B. Xu, Q. M. Zhang, T. Ramotoski, K. A. Wright, and R. Ting, *IEEE T. UFFC* 47 (6), 1296 (2000)
7.  T.-B. Xu, Z-Y. Cheng, and Q. M. Zhang, "High-performance micromachined unimorph actuators based on electrostrictive poly(vinylidede fluoride-trifluoroethylene) copolymer" *Appl. Phys. Lett.* 80 (6), 1082 (2002)
8.  S.F. Liu, S.E. Park, L. E. Cross, and T. R. Shrout, *J. Appl. Phys.* **92 (1)**, 461 (2002)
9.  Z.-Y. Cheng, T.-B. Xu, Q. M. Zhang, R. J. Meyer, D. V. Tol, and J. Hughes, *IEEE T. UFFC* 49 (9), 1312 (2002)
10. J. Nosek, and J. Erhart, *Microelectronic Engineering* 66, 733 (2003)
11. R. A. Walsh, Electromechanical Design Handbook (McGraw-Hill, New York, 2000), P. 5.34.